Journal of Nuclear Materials 386–388 (2009) 227–230

Contents lists available at ScienceDirect

Journal of Nuclear Materials

journal homepage: www.elsevier.com/locate/jnucmat

Multiscale modeling of point defect interactions in Fe–Cr alloys

Kwan L. Wong [a,*], Hyon-Jee Lee [a], Jae-Hyeok Shim [a,b], Babak Sadigh [c], Brian D. Wirth [a]

[a] Nuclear Engineering Department, University of California, Berkeley, CA 94720-1730, USA
[b] Nano-Materials Research Center, Korea Institute of Science and Technology, Seoul 136-791, Republic of Korea
[c] Lawrence Livermore National Laboratory, University of California, Livermore, CA 94551, USA

A B S T R A C T

Predictive performance models of ferritic/martensitic alloys in fusion neutron irradiation environments require knowledge of point defect interactions with Cr, which can be investigated by a multiscale modeling approach. Molecular dynamics simulations, using Finnis–Sinclair-type potentials, have been used to investigate the interstitial diffusion and reveal that the extremes of attractive and repulsive binding between Cr and interstitials change the characteristics of interstitial migration and the Cr-to-Fe diffusivity ratio. *Ab-initio* calculations have been performed to determine the vacancy–Cr interactions, and these calculations reveal complex electronic and magnetic interactions between Cr and Fe. The *ab-initio* values have been used to calculate the Cr-to-Fe diffusivity ratio by a vacancy mechanism using the LeClaire multi-frequency model and a kinetic lattice Monte Carlo model, both of which indicate that Cr diffuses faster than Fe. The modeling results are discussed in the context of the radiation-induced segregation of Cr at grain boundaries in BCC Fe–Cr alloys.

1. Introduction

Fe–Cr alloys are candidate first wall and breeder blanket materials for future Fusion reactors, in addition to candidate fuel cladding, pressure vessel and structural materials for Generation IV reactors [1]. Fundamental understanding of microstructural evolution in these alloys under conditions of fission and fusion neutron irradiation is important, since microstructural changes control mechanical behavior and ultimately, performance.

The observed microstructural evolution of irradiated Fe–Cr alloys include a number of observations that indicate the importance of Cr–point defect interactions, including the non-monotonic dependence of Cr content on irradiation-induced swelling [2,3], complex shifts in the stage I defect recovery processes [4] and short-range ordering at low (<10%) Cr concentrations [5]. Furthermore, there is an indication that Cr segregation behavior under irradiation is more complex than in irradiated austenitic FCC alloys, where Cr depletes at grain boundaries [1,6]. As indicated in Fig. 1, the observed radiation-induced segregation behavior of Cr in ferritic/martensitic Fe–Cr-based alloys and steels involves both enrichment and depletion at grain boundaries, with no clear trend as a function of dose, temperature or Cr content [6]. Enrichment of Cr at grain boundaries can lead to precipitation of secondary phase particles, and negatively affect the mechanical behavior and fracture toughness [1]. Although Cr has been shown to have minimal effect on point defect creation in displacement cascades [7,8], the subsequent diffusion of point defects and their interactions with solutes, impurities, and transmutants ultimately dictates the microstructural evolution and changes in mechanical properties [9–14].

The objective of the present paper is to investigate the interaction of Cr with point defects in BCC Fe–Cr alloys within a hierarchical multiscale framework and to evaluate the diffusivity of Cr and Fe by vacancy and interstitial migration mechanisms. The modeling results will be discussed within the context of the segregation behavior of Cr at grain boundaries.

2. Methodology

Ab-initio calculations have been performed using the Vienna *ab-initio* simulation package (VASP) [15–17]. The Fe and Cr pseudopotentials were taken from the VASP database, within the projector augmented wave (PAW) approach and with plane wave cutoff energies of 334.9 eV for Fe, 283.9 for Cr, and 334.9 eV for the Fe–Cr alloys. The generalized gradient approximation (GGA) is used to describe the exchange correlation functional [18], and the Monkhorst and Pack scheme is used for Brillouin-zone (BZ) sampling [19]. All calculations have simultaneously relaxed the atomic position and the supercell volume (and shape) using the standard conjugate gradient algorithm. The nudged elastic band method [20] is used to determine the migration energies of vacancy exchange with Cr and Fe, as a function of the relative position of the vacancy and Cr atom.

* Corresponding author.
E-mail address: kevwong@socrates.berkeley.edu (K.L. Wong).

0022-3115/$ - see front matter © 2009 Published by Elsevier B.V.
doi:10.1016/j.jnucmat.2008.12.092

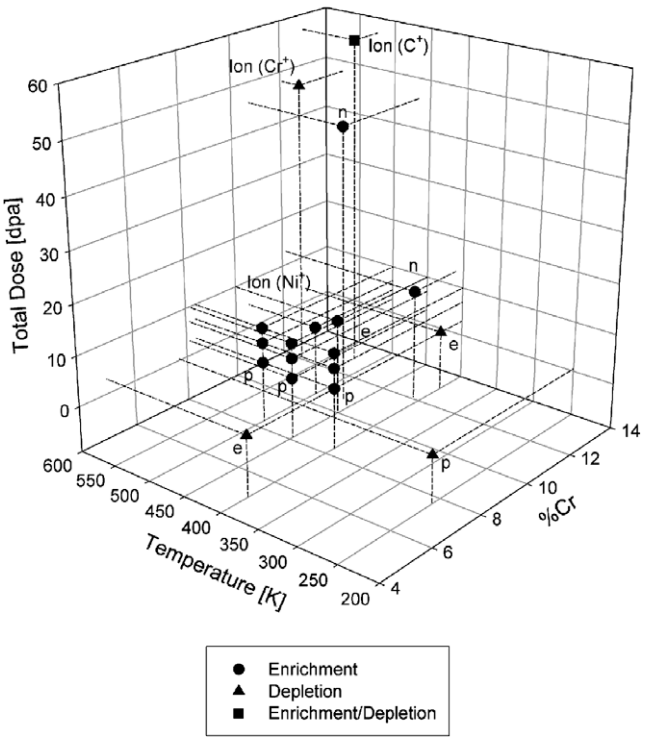

Fig. 1. Summary of experimental data compiled by Faulkner [6] on the radiation-induced segregation in ferritic/martensitic alloys as a function of dose, temperature, Cr content and irradiating particle (n = neutron, p = proton, e = electron).

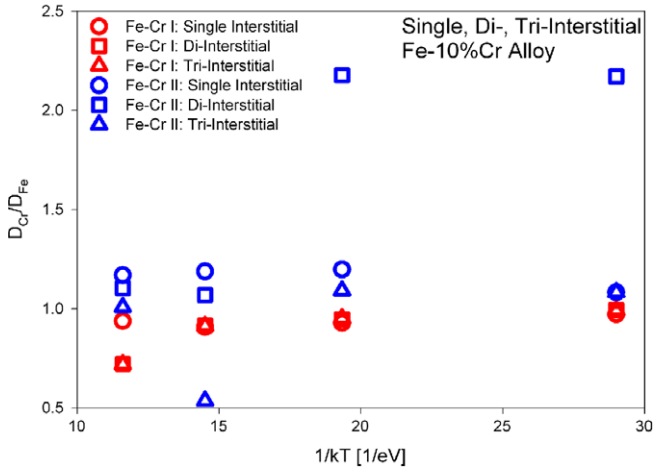

Fig. 2. The ratio of Cr to Fe diffusivity by an interstitial mechanism obtained from MD simulations in a Fe–10%Cr alloy using different interatomic potentials. The diffusivity ratio has been evaluated for single-, di- and tri-interstitials.

Molecular dynamics (MD) simulations of interstitial diffusion in the Fe–Cr alloys have been performed using the semi-empirical, Finnis–Sinclair-type potentials recently fit by Shim et al. [8], which exhibit contrasting Cr interaction fields. The Fe–Cr I potential predicts that Cr is oversized relative to Fe with a compressive strain field and that the binding energy of Cr mixed interstitial dumbbells is negative. The Fe–Cr II potential predicts that undersized Cr with a tensile strain field and positive binding energies for mixed dumbbells [8,21].

Kinetic lattice Monte Carlo (KLMC) simulations were performed in a periodic simulation cell of $60 \times 60 \times 60$ unit cells containing a single vacancy and single Cr atom. This corresponds to the dilute limit with 2.3 atomic parts per million Cr in BCC Fe to evaluate the Cr and Fe diffusivities by a vacancy mechanism. The migration energies obtained from *ab-initio* calculations ($3 \times 3 \times 3$ unit cells, Table 1) were used to define the vacancy exchange probabilities when the vacancy was in the vicinity of a Cr atom, and the specific vacancy–Fe atom exchange was selected at random when not near a Cr atom.

3. Results and discussion

3.1. Fe and Cr diffusivity by an interstitial migration mechanism

Wong et al. have previously shown that using either the Fe–Cr I or Fe–Cr II potential, the effect of Cr solute atoms is to decrease the diffusivity of single interstitials and small clusters of interstitials [21]. Terentyev and Malerba have obtained similar results [22]. The addition of oversized Cr causes the interstitial dumbbells to rotate more frequently to avoid mixed dumbbell formation; in contrast, the positive binding of mixed dumbbells traps interstitials at the undersized Cr and hinders long translational jumps. Here, we have extended the previous work by calculating the ratio of Cr-to-Fe diffusivity by an interstitial mechanism. Fig. 2 plots the ratio of the Cr and Fe diffusivities in a Fe–10%Cr alloy obtained with a single, di- and tri-interstitial for the Fe–Cr I and Fe–Cr II potentials. The results are consistent with the binding energies, namely that the Fe–Cr I potential predicts that Cr is a slower diffuser than Fe when Cr is oversized (repulsive interaction with the interstitial). In contrast, when Cr is undersized/attractive in FeCr II, Cr diffuses faster than Fe by 10–30%, as a consequence of mixed dumbbell formation and Cr–interstitial dumbbell binding energy. The Fe–Cr II potential is consistent with the size effects and interstitial binding energies for Cr atoms in BCC Fe–Cr alloys predicted by *ab-initio* calculations [23], and thus the preliminary conclusion of these MD simulations is that Cr diffuses faster than Fe by an interstitial mechanism. Faster diffusivity of Cr by an interstitial mechanism is consistent with an inverse Kirkendall-based model [13] of Cr dragging by interstitials, which would produce Cr enrichment at the dominant interstitial sinks in the microstructure. However, quantifying the predicted levels of Cr enrichment will require more precise values of the Cr and Fe diffusivities by interstitial and interstitial cluster mechanisms, including the use of more recent potentials developed for Fe [24] in addition to determining the partitioning of interstitial-type defect fluxes to dislocation and grain boundary sinks.

3.2. Vacancy–Cr interactions in BCC Fe–Cr alloys

The VASP *ab-initio* calculations predict a reference state of pure Fe that is ferromagnetic BCC with a lattice parameter of 0.283 nm and a magnetic moment of $2.19\mu_B$, while the Cr ground state is an anti-ferromagnetic BCC structure with a lattice parameter of 0.285 nm and a magnetic moment of $\pm 1.09\mu_B$, which are consistent

Table 1
Migration energy barrier (eV) corresponding to the vacancy–atom exchanges for a vacancy in proximity to a Cr solute atom in the BCC lattice, following LeClaire's definition [27].

	ω_0	ω_2	ω_3	ω_4	ω_3'	ω_4'	ω_3''	ω_4''	ω_5	ω_6
$(2 \times 2 \times 2)$	0.61	0.56	0.68	0.57	0.65	0.55	0.47	0.63		
$(3 \times 3 \times 3)$	0.66	0.52	0.66	0.62	0.65	0.59	0.60	0.57	0.74	0.69

with both experimental observations [25] and previous *ab-initio* calculations by Olsson [23,26]. In the Fe–Cr alloys, the magnetic moment and atomic size of the Cr atoms depend strongly on the alloy Cr content. At Cr concentrations below 16.7%, Cr is strongly anti-ferromagnetic, and the excess atomic volume of the system is positive for Cr concentrations up to 25%, suggesting that Cr is oversized in Fe matrix. However, careful examination of the 1st NN Fe atoms indicates relaxation toward the Cr atom, indicating that Cr is undersized. This apparent difference in the observed Cr atomic volume can be rationalized by comparing with the relaxation near a vacancy, in which oscillating expansion and contraction of NN shells occurs. In this case, the total relaxation over all NN shells produces an increase in the system volume even for an undersized species. Thus, our calculations indicate that Cr is an undersized solute with a surrounding tensile field and therefore should not be expected to bind with a vacancy. However, the further *ab-initio* results show that the binding energy of a vacancy and a first NN Cr atom is about 0.05 eV, which is likely caused by electronic and magnetic interactions. For example, when Cr is paired with a vacancy in a Fe–1.8%Cr alloy, the magnetic moment on the Cr decreases from -1.88 to $-2.12\mu_B$, while the magnetic moment on the 1st NN Fe atoms increases from 2.2 to $2.4\mu_B$.

The activation energy from our VASP calculations for vacancy exchange with Fe in pure BCC Fe is 0.66 eV, whereas it is 0.52 eV for the direct exchange with a Cr atom in a Fe–1.9%Cr alloy. This suggests a faster diffusivity for Cr relative to Fe due to both vacancy binding and preferential vacancy exchange. However, since solute diffusion in BCC alloys is controlled by more than just the direct vacancy exchange, we have followed the multi-frequency models developed by LeClaire [27,28] to calculate the activation energies of vacancy–atom exchanges for a vacancy in close proximity to Cr. The resulting vacancy migration energies are presented in Table 1 for simulation cells containing $2 \times 2 \times 2$ (Fe–6%Cr) and $3 \times 3 \times 3$ (Fe–1.9%Cr) unit cells.

3.3. Self-diffusivity of Fe and Cr from vacancy migration

The self-diffusivity of Fe in BCC Fe was calculated using the LeClaire model [27,28], based on the values presented in Table 1 and values for the vacancy formation and migration energy ($E^{v,m}$ = 0.65 eV, $E^{v,f}$ = 2.18 eV) obtained from *ab-initio* calculations. This results in a predicted diffusivity given by Eq. (1),

$$D^{Fe}_{BCC-Fe} = 2.051 \cdot 10^{-5} \times \exp\left(-\frac{2.84}{k_B T}\right) [m^2/sec]. \quad (1)$$

This value for the Fe self-diffusivity is consistent with the range of values previously obtained by Becquart and Domain [29,30].

Similarly, the Cr diffusivity has been calculated from the LeClaire model [27,28] using the values presented in Table 1. For this calculation, it is assumed that the various jump frequencies are determined by the activation free energies with an invariant pre-exponential factor (ν_o), given the similar atomic size and mass of Cr and Fe, although there may be effects of Cr on the vacancy migration entropy and the vibrational density of states at the saddle point that are not included in this assumption. Thus, in the dilute limit, the Cr diffusion coefficient is:

$$D^{Cr}_{BCC-Fe} = a^2 w_2 f_2 \frac{w'_4}{w'_3} c^{eq}_v, \quad (2)$$

where

$$f_2 = \frac{1+t_1}{1-t_1},$$
$$t_1 = -\frac{w_2}{w_2 + 3w_3 + 3w'_3 + w''_3 - \frac{w_3 w_4}{w_4 + F w_5} - \frac{2w'_3 w'_4}{w'_4 + 3F w_0} - \frac{w''_3 w''_4}{w''_4 + 7F w_0}}, \quad (3)$$

and F = 0.512. For concentrated alloys, the Fe self-diffusivity will be modified by the presence of Cr atoms, which has been determined [27,28] to follow:

$$D^{Fe}_{BCC-Fe}(c_{Cr}) = D^{Fe}_{BCC-Fe}(c_{Cr} = 0)(1 + b c_{Cr}), \quad (4)$$

where b is a solute enhancement factor. Assuming the effect of the solute is not sufficiently strong to alter the solvent correlation factor f appreciably from the value f_0 in pure solvent,

$$b = -20 + \frac{1}{w_0}\left[(3w'_3 + w'' + 3w_3)\frac{w'_4}{w'_3} + (3w_4 + 3w_5)\frac{w_6}{w_5} + 3w'_4 + w''_4 + 3w_6\right]. \quad (5)$$

From the above equations, the ratio between the Cr and Fe diffusivity is obtained as:

$$\frac{D^{Cr}_{BCC-Fe}}{D^{Fe}_{BCC-Fe}(c_{Cr})} = \frac{w_2}{w_0}\frac{f_2}{f_0}\frac{w'_4}{w'_3}\frac{1}{(1 + b c_{Cr})}. \quad (6)$$

The ratio between Cr and Fe diffusivities in BCC Fe–Cr alloys obtained from Eq. (6) are plotted in Fig. 3 as a function of temperature. The results predict that Cr is a much faster diffuser than Fe, both in the dilute limit (solid line) and when including the solute enhancement of solvent diffusion in a concentrated Fe–10%Cr alloy (dashed line). KLMC simulations have also been performed to evaluate the ratio of Cr to Fe diffusivity. In these simulations, the values of vacancy jump migration energies modified when near a Cr solute atom presented in Table 1 have been used to determine the specific vacancy–atom exchanges, assuming an invariant jump frequency pre-factor. The KLMC simulation results, plotted as filled symbols in Fig. 3, predict that Cr diffuses much faster than Fe and in fact, with much larger ratios than predicted by the LeClaire model but with a similar temperature dependence as the dilute limit LeClaire model prediction. The clear conclusion from this analysis is that Cr will diffuse faster (~2–150 times larger) than Fe by a vacancy mechanism, and that it appears that the relative ratio of Cr to Fe is much larger for a vacancy than an interstitial mediated diffusion mechanism. Within an inverse Kirkendall model of radiation-induced segregation [13], the faster diffusivity of Cr by a vacancy mechanism would produce Cr at grain boundaries.

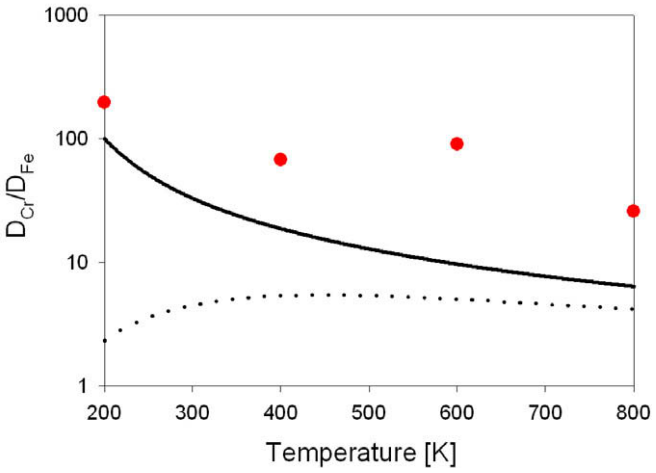

Fig. 3. The ratio of Cr to Fe diffusivity by a vacancy mechanism, as calculated based on *ab-initio* simulations of the vacancy–atom exchange energies implemented into the multiple frequency LeClaire model [27,28] in the dilute limit (solid line), as compared to KLMC simulations (data points). As well as, the effect of solute enhancement of Fe self-diffusion in the LeClaire model in an Fe–10%Cr alloy is shown with the dotted line.

4. Conclusions

A hierarchical multiscale modeling approach has been used to evaluate Cr interactions with point defect clusters in BCC Fe–Cr alloys. *Ab-initio* calculations of vacancy–Cr binding energy and the activation energy for vacancy–atom exchanges in the proximity of Cr have been used to calculate the diffusivities of Fe and Cr by a vacancy mechanism in the LeClaire multiple frequency model and kinetic lattice Monte Carlo simulations. This analysis leads to the conclusion that Cr diffuses much faster (~2–150 times larger) than Fe by a vacancy mechanism. The relative diffusivity of Cr to Fe by an interstitial mechanism has been investigated using molecular dynamics simulations, with two different Fe–Cr potentials that predict either an attractive or a repulsive interaction between Cr and the interstitial defects. The potential predicting an attractive interaction of Cr with interstitials (Fe–Cr II) is more consistent with *ab-initio* predictions, and for this case, the Cr diffusivity by an interstitial mechanism is between 10% and 30% larger than Fe diffusivity. Thus, it seems apparent that either Cr enrichment or depletion at grain boundaries could be expected under irradiation, depending on the relative fluxes of interstitial versus vacancy defects. Future efforts will focus on developing atomic-scale models of Cr transport based on vacancy and interstitial-type diffusion mechanisms and on evaluating the relative point defect fluxes to various microstructural sinks to better understand the apparently contradictory experimental observations of Cr segregation in irradiated ferritic/martensitic alloys.

Acknowledgements

This work has been supported by the Office of Fusion Energy Sciences, US Department of Energy, under Grant DE-FG02-04ER54750.

References

[1] R.L. Klueh, D.R. Harries, High Chromium ferritic and Martensitic Steels for Nuclear Application, ASTM MONO3, ASTM, West Conshohocken, PA, 2001.
[2] E.A. Little, D.A. Stow, J. Nucl. Mater. 87 (1979) 25.
[3] F.A. Garner, M.B. Toloczko, B.H. Sencer, J. Nucl. Mater. 276 (2000) 123.
[4] F. Maury, P. Lucasson, A. Lucasson, F. Faudot, J. Bigot, J. Phys. F: Met. Phys. 17 (1987) 1143.
[5] I. Mirebeau, M. Hennion, G. Parette, Phys. Rev. Lett. 53 (1984) 537.
[6] Z. Lu, R.G. Faulkner, G.S. Was, Scripta Mater., submitted for publication.
[7] D.A. Terentyev, L. Malerba, R. Chakarova, K. Nordlund, P. Olsson, M. Rieth, J. Wallenius, J. Nucl. Mater. 349 (2006) 119.
[8] J.-H. Shim, H.-J. Lee, B.D. Wirth, J. Nucl. Mater. 351 (2006) 56.
[9] G.R. Odette, J. Nucl. Mater. 85 & 86 (1979) 533.
[10] L.K. Mansur, E.E. Bloom, J. Metals 34 (1982) 23.
[11] B.N. Singh, A.J.E. Foreman, J. Nucl. Mater. 122 & 123 (1984) 537.
[12] L.K. Mansur, E.H. Lee, P.J. Maziasz, A.F. Rowcliffe, J. Nucl. Mater. 141–143 (1986) 633.
[13] G.S. Was, S.M. Bruemmer, J. Nucl. Mater. 216 (1994) 326.
[14] R. Schaublin, P. Spatig, M. Victoria, J. Nucl. Mater. 258–263 (1998) 1178.
[15] G. Kresse, J. Hafner, Phys. Rev. B 47 (1993) 558.
[16] G. Kresse, J. Furthmuller, Phys. Rev. B 54 (1996) 11169.
[17] G. Kresse, J. Furthmuller, Comput. Mater. Sci. 6 (1996) 15.
[18] J.P. Perdew, K. Burke, M. Ernzerhof, Phys. Rev. Lett. 77 (1996) 3865.
[19] H.J. Monkhorst, J.D. Pack, Phys. Rev. B 13 (1976) 5188.
[20] G. Henkelman, H. Jonsson, J. Chem. Phys. 113 (2000) 9978.
[21] K.L. Wong, J.-H. Shim, B.D. Wirth, J. Nucl. Mater. 367–370 (2007) 276.
[22] D. Terentyev, L. Malerba, J. Nucl. Mater. 329 (2004) 1161.
[23] Par Olsson, Thesis (2006).
[24] G.J. Ackland, M.I. Mendelev, D.J. Srolovitz, S.W. Han, A.V. Barashev, J. Phys. Condens. Mater. 16 (2004) S2629.
[25] C. Kittel, Introduction to Solid State Physics, eighth Ed., John Wiley, Hoboken, NJ, 2005.
[26] J. Wallenius, P. Olsson, C. Lagerstedt, N. Sandbers, R. Chakarova, V. Pontikis, Phys. Rev. B. 69 (2004) 094103.
[27] A.D. LeClaire, Philos. Mag. 21 (1970) 819.
[28] A.D. LeClaire, J. Nucl. Mater. 69 (1978) 70.
[29] C. Domain, C.S. Becquart, PRB 71 (2005) 214109.
[30] C.S. Becquart, C. Domain, NIMB 202 (2003) 44.